



Recruitment of CG-NAP to the Golgi apparatus through interaction with dynein-dynactin complex

Kim, Hon-Song
Takahashi, Mikiko
Matsuo, Kazuhiko
Ono, Yoshitaka

(Citation)

Genes to Cells, 12(3):421-434

(Issue Date)

2007-03-05

(Resource Type)

journal article

(Version)

Accepted Manuscript

(URL)

<https://hdl.handle.net/20.500.14094/90000959>



Recruitment of CG-NAP to the Golgi apparatus through interaction with dynein-dynactin complex

Hon-Song Kim¹, Mikiko Takahashi^{2*}, Kazuhiko Matsuo¹, and Yoshitaka Ono^{1,2}

¹Graduate School of Science and Technology

²Biosignal Research Center, Kobe University, Kobe 657-8501, Japan

Running title: Recruitment of CG-NAP to the Golgi

*Correspondence: Mikiko Takahashi

Phone: +81-78-803-5473

Fax: +81-78-803-5782

E-mail: tmikiko@kobe-u.ac.jp

Total character count of this paper: 45736 characters

Abstract

The structural organization and position of the Golgi apparatus are highly regulated by microtubule cytoskeleton and microtubule motor proteins. The mechanisms linking these proteins to the Golgi apparatus remain elusive. Here, we found that CG-NAP (centrosome and Golgi-localized PKN associated protein) was localized to the Golgi apparatus in a microtubule-dependent manner. Microtubule-binding experiments revealed that CG-NAP possessed two microtubule-binding domains. We also found that CG-NAP was well-colocalized with cytoplasmic dynein subunits during recovery from the on-ice treatment of cells that induced dissociation of CG-NAP from the Golgi. Similar colocalization was observed during recovery from the acetate treatment, which has been reported to inhibit the dynein-mediated transport. CG-NAP was coimmunoprecipitated with a dynactin subunit p150^{Glued}. Expressing the p150^{Glued}-binding region of CG-NAP fused with mitochondria-targeting sequence induced recruitment of mitochondria to the pericentriolar area, suggesting that this region interacts with functional cytoplasmic dynein *in vivo*. Moreover, overexpression of this region caused fragmentation of the Golgi similar to that of dynamitin. These results suggest that CG-NAP is recruited to the minus ends of microtubules by interacting with cytoplasmic dynein, thereby localizes to the Golgi apparatus in a microtubule-dependent manner, and possibly involved in the formation of the Golgi near the centrosomes.

Introduction

In non-polarized mammalian cells the Golgi apparatus is a single copy dynamic organelle localized around the centrosome and actively maintained there. The Golgi apparatus plays a central role in membrane transport pathway by receiving the cargo packaged into membrane vesicles from the endoplasmic reticulum (ER), and sorting them to the plasma membrane or the endocytic pathway. Simultaneously, membrane components are transported back to the ER as vesicles and tubules. These dynamic and bidirectional flow of cargoes between ER and the Golgi is crucial to maintaining the structure and function of the Golgi apparatus and its location near the centrosome (Burkhardt 1998; Rios *et al.* 2003). It is now clear that this flow is dependent on both microtubule cytoskeleton and microtubule motor proteins. However, the mechanism linking microtubules and motor proteins to the Golgi apparatus remains elusive.

Cytoplasmic dynein, a multi subunits complex consisting of two heavy chains and several intermediate, light intermediate and light chains, is a minus end-directed microtubule motor protein involved in multiple cellular functions including mitosis, maintenance of the Golgi apparatus and intracellular transport (Karcher *et al.* 2002; Karki *et al.* 1999). In membrane transport, cytoplasmic dynein is thought to act in transport from ER and endosomes to the minus ends of microtubules (King 2000). Dynactin is a large multi subunit complex including p150^{Glued}, dynamitin, p24 and ARP1 subunits (Allan 1996; Holleran *et al.* 1998; Karki and Holzbaaur 1999) that stimulate cytoplasmic dynein-mediated movement in vitro (Schroer *et al.* 1991). Among them, p150^{Glued}, the mammalian homolog of the product of the *Drosophila* gene *Glued* (Holzbaaur *et al.* 1991), binds to both microtubules (Waterman-Storer *et al.* 1995) and cytoplasmic dynein (Gill *et al.* 1991). It was also reported that overexpression of dynamitin disrupts dynein-cargo interaction, thereby inducing fragmentation of the Golgi apparatus (Burkhardt *et al.* 1997; Echeverri *et al.* 1996). Thus, dynactin mediates the binding of dynein to membranous cargoes. However, detailed

molecular mechanisms for interaction of dynactin and their cargo are poorly understood.

A giant anchoring protein CG-NAP (Takahashi *et al.* 1999), also known as AKAP350 (Schmidt *et al.* 1999), AKAP450 (Witczak *et al.* 1999) or AKAP9, localizes to centrosomes throughout the cell cycle and the Golgi apparatus at interphase. CG-NAP has been found to anchor various signaling molecules such as protein kinase A (PKA), PKN, protein phosphatase 1, protein phosphatase 2A, phosphodiesterase 4D, calmodulin, casein kinase 1 δ/ϵ , cdc42 interacting protein 4 (CIP4), Ran, and Cyclin E/Cdk2 (Keryer *et al.* 2003; Larocca *et al.* 2004; Nishimura *et al.* 2005; Sillibourne *et al.* 2002; Takahashi *et al.* 1999; Takahashi *et al.* 2002). Thus, CG-NAP may coordinate the location and activity of these enzymes to regulate the phosphorylation states of specific substrates at the centrosome and the Golgi apparatus. We have found that CG-NAP is localized to the centrosome via the carboxyl-terminal region and serves as microtubule nucleation sites by anchoring γ -tubulin ring complex (γ -TuRC) at the centrosome (Takahashi *et al.* 2002). Furthermore, suppression of CG-NAP expression by RNA interference alters the Golgi morphology (Larocca *et al.* 2004). However, the mechanism for this alteration as well as for the localization of CG-NAP to the Golgi remains to be determined.

Here we demonstrated that CG-NAP localized to the Golgi apparatus in a microtubule-dependent manner, and CG-NAP was well-colocalized with dynein-dynactin subunits on the microtubules during recovery both from the on-ice and acetate treatments. Endogenous CG-NAP interacted with p150^{Glued}, and expression of p150^{Glued}-binding region of CG-NAP fused with mitochondria-targeting sequence induced recruitment of mitochondria to pericentriolar area, suggesting that this region interacts with functional cytoplasmic dynein *in vivo*. Furthermore, overexpression of this region caused fragmentation of the Golgi probably by sequestering the cytoplasmic dynein to cytosol. These results imply that CG-NAP is recruited to the Golgi apparatus by interacting with cytoplasmic dynein, and possibly involved in the organization and maintenance of the Golgi apparatus.

Results

CG-NAP localizes to the Golgi apparatus in a microtubule-dependent manner.

To investigate the Golgi-targeting mechanism of CG-NAP, we examined subcellular localization of CG-NAP after various treatments. Among them, when the cells were placed on ice for 30 minutes, we found that CG-NAP disappeared from the Golgi apparatus and only centrosome-localized CG-NAP was observed (Fig. 1A, c). Under this condition, microtubules were depolymerized (Fig. 1A, d), and the Golgi apparatus represented relatively loose shape (Fig. 1A, h). When the cells were incubated again at 37°C for 20 minutes microtubules were repolymerized (Fig. 1A, f), and CG-NAP was relocated to the Golgi (Fig. 1A, e). CG-NAP dissociation from the Golgi by the on-ice treatment was suppressed in the presence of taxol, a microtubule stabilizing agent (Fig. 1B, i). Furthermore, nocodazole, a microtubule depolymerizing agent, suppressed CG-NAP relocation to the Golgi apparatus after recovery from the on-ice treatment (Fig. 1B, k). These results indicate that CG-NAP localizes to the Golgi apparatus in a microtubule-dependent manner.

CG-NAP associates with microtubules.

To further characterize the Golgi-targeting mechanism of CG-NAP, we investigated the process during recovery from the on-ice treatment. To visualize cytoskeleton-associated proteins clearly, cells were briefly extracted with detergent prior to fixation. After 4 minutes from recovery, microtubules were nucleated from the centrosomes to form asters (Fig. 2A, b). At this time point, CG-NAP was detected along with the microtubule asters (Fig. 2A, a). After 7 minutes, the amount of microtubule-associated CG-NAP was increased (Fig. 2A, d) in conjunction with elongating microtubule asters (Fig. 2A, e). After 20 minutes, when the microtubule network became nearly normal (Fig. 2A, h), microtubule-associated CG-NAP was barely detectable and only pericentriolar staining was observed (Fig. 2A, g). Similar results were obtained with both HeLa cells and the cells recovered from nocodazole treatment

(our unpublished results). These results suggest that CG-NAP is recruited to the microtubules until relocating to the Golgi apparatus.

Next, to examine whether endogenous CG-NAP can bind microtubules, we performed microtubule-binding assay. As shown in Figure 2B, endogenous CG-NAP was efficiently co-sedimented with polymerized microtubules as well as other microtubule-interacting proteins, such as GMAP-210 and p150^{Glued}, indicating that CG-NAP can bind microtubules. To identify the microtubule binding domain in the CG-NAP, we performed similar assay using cell lysates expressing deletion mutants. Figure 2C shows schematic representation of the deletion mutants used in this paper. In the text, deletion mutants are designated as CG-NAP_{X-X}, where X-X represents amino acid residues. As shown in Figure 2D, FLAG-tagged deletions, CG-NAP₁₂₂₉₋₁₉₁₇ and CG-NAP₂₈₇₅₋₃₈₉₉, were co-sedimented with microtubules in the presence of taxol, suggesting that CG-NAP associates with microtubules via these two regions.

CG-NAP colocalizes with dynein-dynactin subunits during recovery from the on-ice treatment.

At 4~7 minutes after recovery from the on-ice treatment, CG-NAP was not colocalized with entire length of microtubules (Fig. 2A). CG-NAP represented continuous dot-like staining pattern along the microtubules, which is reminiscent of the distribution of motor proteins. Therefore, we compared the localization of CG-NAP with cytoplasmic dynein subunits at 4 minutes after recovery. As shown in Figure 3, microtubule-associated CG-NAP was well-colocalized with dynamitin, p150^{Glued}, and dynein intermediate chain (DIC). These colocalization patterns persisted until CG-NAP localized mostly to the Golgi apparatus (our unpublished results). These results suggest that CG-NAP is recruited to the microtubules by dynein-dynactin complex.

CG-NAP colocalizes with dynein-dynactin subunits during recovery from acetate treatment.

Brief acetate treatment, which leads to cytoplasmic acidification, has been known to induce redistribution of several organelles including lysosomes (Heuser 1989), endosomes (Parton *et al.* 1991) and the Golgi apparatus (Vaughan *et al.* 1999). Though detailed mechanism has been elusive, it has been thought that dynactin-vesicle interaction is disrupted under this condition (Vaughan *et al.* 1999). After removal of acetate, dynein-mediated motility is initiated, and then those organelles are reformed. We examined CG-NAP behavior under this condition. In control cells, CG-NAP was mainly detected at pericentriolar area and only a faint amount was colocalized with microtubules (Fig. 4A). After 15 minutes exposure to acetate, Golgi apparatus exhibited slight diffusion, monitored by anti GM130 antibody (Fig. 4B). CG-NAP exhibited diffused localization surrounded by vesicle-like staining along microtubules. At 4 minutes after acetate wash out, CG-NAP was partially colocalized with radial microtubules, which was well-colocalized with dynamitin (Fig. 4C). CG-NAP was also well-colocalized with DIC along microtubules (our unpublished results). Thirty minutes later, CG-NAP became relocalized to the Golgi apparatus in accordance with the decrease in microtubule-associated fractions (Fig. 4D), which was coincided with the distribution of dynamitin. These results again suggest that CG-NAP is transported along microtubules by cytoplasmic dynein, thereby localizes to the Golgi apparatus.

CG-NAP associates with dynactin subunit, p150^{Glued}.

To investigate whether CG-NAP associates with cytoplasmic dynein complex, we performed coimmunoprecipitation study of endogenous proteins. Among several subunits examined, p150^{Glued} was found to be coimmunoprecipitated with CG-NAP by anti CG-NAP antibody from HeLa cell extracts (Fig. 5A). Furthermore, the interaction was also observed between FLAG-CG-NAP and HA-p150^{Glued} exogenously expressed in COS7 cells (Fig. 5B). To

identify the domains of CG-NAP responsible for this interaction, we performed coimmunoprecipitation study using cell extracts coexpressing various FLAG-tagged deletion mutants of CG-NAP (see Fig. 2C) and HA-tagged p150^{Glued}. HA-p150^{Glued} was reciprocally coimmunoprecipitated with either FLAG-CG-NAP₁₂₂₉₋₁₉₁₇ or CG-NAP₂₈₇₅₋₃₈₉₉ (Fig. 5C). The interaction of HA-p150^{Glued} with FLAG-CG-NAP₁₂₂₉₋₁₉₁₇ was stronger than that with FLAG-CG-NAP₂₈₇₅₋₃₈₉₉. These results suggest that CG-NAP can associate with p150^{Glued} through amino acid residues 1229-1917 or 2875-3899.

CG-NAP₁₂₂₉₋₂₄₄₄ can be loaded onto the minus end-directed transport by cytoplasmic dynein.

Next, we monitored subcellular localization of these deletion mutants. Since we have already shown that CG-NAP₂₈₇₅₋₃₈₉₉ is localized to the centrosomes (Takahashi *et al.* 2002), we focused on the distribution of CG-NAP₁₂₂₉₋₁₉₁₇. Unexpectedly, FLAG-CG-NAP₁₂₂₉₋₁₉₁₇ was mainly localized in the cytoplasm and, in part, at pericentriolar region (Fig. 6A), suggesting that this region cannot be efficiently transported to the minus ends of microtubules by cytoplasmic dynein. When a longer fragment FLAG-CG-NAP₁₂₂₉₋₂₄₄₄ was expressed, it was detected at pericentriolar area, whereas the extended region FLAG-CG-NAP₁₉₁₇₋₂₄₄₄ was distributed in the cytoplasm (Fig. 6A). To examine the localization of these deletions more clearly, we fused them with mitochondria-targeting sequence (Mt) of the D-AKAP1 (see Experimental Procedures). D-AKAP1 is an A-kinase anchoring protein that binds and targets PKA to the outer mitochondrial membranes (Ma *et al.* 2002), and thus we expected that expression of Mt-tagged deletions of CG-NAP alter the mitochondrial distribution. As a control, we fused Mt sequence to the amino terminus of GFP (Mt-GFP), which was colocalized with mitochondria throughout the cytoplasm (Fig. 6B, a), and had no effect on mitochondrial distribution (Fig. 6B, b). Mt-FLAG-CG-NAP₁₂₂₉₋₂₄₄₄ exhibited pericentriolar localization (Fig. 6B, c). Furthermore, it caused drastic alteration of mitochondrial

distribution from cytoplasm to the pericentriolar area (Fig. 6B, d), suggesting that this region can be efficiently loaded onto minus end-directed transport. On the other hand, neither Mt-FLAG-CG-NAP₁₂₂₉₋₁₉₁₇ nor Mt-FLAG-CG-NAP₁₉₁₇₋₂₄₄₄ could change the mitochondrial distributions (Fig. 6B, f and h). Since the fragment FLAG-CG-NAP₁₂₂₉₋₂₄₄₄ was not colocalized with endogenous CG-NAP at the Golgi apparatus (our unpublished results), this region may mediate constitutive transport of CG-NAP to the minus ends of microtubules from cytosol before association with the Golgi apparatus that may need additional region. Next we examined whether the fragment CG-NAP₁₂₂₉₋₂₄₄₄ can associate with microtubules and p150^{Glued} more tightly than CG-NAP₁₂₂₉₋₁₉₁₇. FLAG-CG-NAP₁₂₂₉₋₂₄₄₄ also interacted with both microtubules (Fig. 6C) and p150^{Glued} (Fig. 6D), however, at almost similar levels to FLAG-CG-NAP₁₂₂₉₋₁₉₁₇, implying that efficient loading of CG-NAP₁₂₂₉₋₂₄₄₄ to the minus end-directed transport is not mediated by a stronger interaction with p150^{Glued} and/or microtubules but by some additional mechanism(s). These results suggest that the region comprising amino acids 1229-2444 is responsible for the minus end-directed transport of CG-NAP by cytoplasmic dynein complex *in vivo*.

Overexpression of CG-NAP₁₂₂₉₋₂₄₄₄ causes fragmentation of the Golgi apparatus similar to that of dynamitin.

Finally, we examined the effect of overexpression of FLAG-CG-NAP₁₂₂₉₋₂₄₄₄ on the organization of the Golgi apparatus. Cells overexpressing FLAG-CG-NAP₁₂₂₉₋₂₄₄₄ exhibited fragmented Golgi structures monitored by anti-GM130 antibody (Fig. 7A), which was similar to the effect of dynamitin overexpression (Fig. 7B). Dynamitin overexpression is known to disrupt cytoplasmic dynein complex, resulting in the fragmentation of the Golgi apparatus to form mini-stacks maintaining *cis*- and *trans*-organization (Fig. 7B). To examine whether the scattered Golgi structures within the cells overexpressing FLAG-CG-NAP₁₂₂₉₋₂₄₄₄ also form such mini-stacks, we monitored the localization of GM130 and golgin 97, *cis*- and

trans-Golgi proteins, respectively. These two proteins were detected at adjacent but distinct positions in the same Golgi fragments (Fig. 7A right, magnified images) similar to those in dynamin-overexpressing cells (Fig. 7B right, magnified images), suggesting that FLAG-CG-NAP₁₂₂₉₋₂₄₄₄ overexpression inhibits the cytoplasmic dynein function. To investigate whether this was caused by sequestering p150^{Glued}, we monitored the localization of p150^{Glued} (Fig. 7C). As reported previously (Vaughan *et al.* 1999), microtubule-associated p150^{Glued} was unaffected by dynamin overexpression (Fig. 7C bottom, magnified image). On the other hand, in the cells overexpressing FLAG-CG-NAP₁₂₂₉₋₂₄₄₄ p150^{Glued} was displaced from the radial microtubules (Fig. 7C top, magnified images). These results suggest that overexpression of FLAG-CG-NAP₁₂₂₉₋₂₄₄₄ causes fragmentation of the Golgi by sequestering p150^{Glued}, and presumably intact cytoplasmic dynein complex, involved in the organization of the Golgi apparatus.

Discussion

We have demonstrated that CG-NAP is loaded onto minus end-directed transport by interacting with cytoplasmic dynein until localizing to the Golgi apparatus. Although, the transport of CG-NAP along microtubules could not be detected at steady state, that was clearly observed during recovery from either on-ice treatment (Fig. 3) or acetate treatment (Fig. 4). It was demonstrated that cytoplasmic dynein can be visualized along microtubule arrays when cells are briefly treated at room temperature prior to fixation (Vaughan *et al.* 1999). The authors suggested that this condition serves to isolate normally undetectable kinetic intermediates in the initiation of dynein-based motility. Likewise, recovering the cells from treatments we have employed here may enable us to detect synchronized movement of CG-NAP together with cytoplasmic dynein along microtubules.

CG-NAP interacted with a dynactin subunit p150^{Glued} through amino acid residues 1229-1917 (Fig. 5C), however, this region was not sufficient but additional carboxyl-terminal region (amino acid residues 1918-2444) was required for loading onto the minus end-directed transport by cytoplasmic dynein (Fig. 6). Furthermore, overexpression of this longer fragment (amino acid residues 1229-2444) caused fragmentation of the Golgi. At the initial stage of cargo transport tethering of cargo to microtubule is mediated by dynactin complex through microtubule binding domain of p150^{Glued}, and then dynein complex is recruited to dynactin complex followed by switching the microtubule binding domain from p150^{Glued} to dynein heavy chain to initiate transport. This switching was reported to be triggered by phosphorylation of p150^{Glued} by PKA (Vaughan *et al.* 2002). CG-NAP is an A-kinase anchoring protein (AKAP) having two RII-binding domains (Takahashi *et al.* 1999), one of which is located in the p150^{Glued}-binding region (amino acid residues 1229-1917). Nevertheless, this fragment was not sufficient to elicit minus end-directed transport. One possibility is that the latter region (amino acid residues 1918-2444 of CG-NAP) plays a role in recruiting dynein complex and/or facilitating the formation of dynein-dynactin complex

although the association of this region with dynein subunits has not been detected thus far. Another possibility is that the latter region is required for maintaining the phosphorylation states of p150^{Glued} for proper complex formation. In addition, it was reported that CG-NAP/AKAP350 associates with CIP4 at the Golgi apparatus through amino acid residues 1076-2143 of AKAP350 (Larocca *et al.* 2004), which corresponds to 1452-2519 of CG-NAP overlapping with the region (amino acid residues 1229-2444) elicited the minus end-directed transport. Larocca *et al.* also presented that overexpression of CIP4 binding region of CG-NAP/AKAP350 or suppression of CG-NAP/AKAP350 by RNA interference alters the Golgi morphology (Larocca *et al.* 2004). It is possible that this alteration was caused by inhibiting cytoplasmic dynein function but not by sequestering CIP4, or by combined effect of sequestering both cytoplasmic dynein and CIP4. CIP4 might be involved in the formation of the complex mediating the minus ends-directed transport of CG-NAP along microtubules. Further studies will be needed to address these possibilities.

CG-NAP remains at centrosomes under various conditions, such as on-ice treatment (Fig. 1), and nocodazole treatment (Takahashi *et al.* 1999), suggesting the microtubule-independency in localization to the centrosomes. However, centrosomal CG-NAP may also be recruited by cytoplasmic dynein before stable attachment to centrosomes through centrosome-targeting domain (Gillingham *et al.* 2000; Takahashi *et al.* 2002). Pericentrin, sharing homology with CG-NAP (Takahashi *et al.* 2002), was demonstrated to interact with dynein light intermediate chain 1 and be recruited to centrosomes in a cytoplasmic dynein-dependent manner (Tynan *et al.* 2000; Young *et al.* 2000), supporting this idea. Further, dynamin overexpression caused the reduction of centrosomal CG-NAP (our unpublished results), suggesting that both centrosome and Golgi-localized CG-NAP are recruited to the minus ends of microtubules by cytoplasmic dynein followed by steady-state localization to these organelles. If this is the case, it will be of interest to elucidate the mechanism how these two destinations are determined during

transport of CG-NAP as a cargo.

It has been clear that the Golgi apparatus is dependent on microtubules for its static maintenance as a single organelle near the centrosome as well as for its dynamic formation via vesicular transport. Several non-motor microtubule-binding proteins have been proposed as linkers between Golgi membranes and microtubules. A *cis*-Golgi microtubule binding protein GMAP210 was proposed to recruit γ -TuRC to the Golgi membranes to nucleate short microtubules and contribute to the assembly and maintenance of the Golgi around the centrosome (Rios *et al.* 2004), however, several contradictory evidences were presented (Barr *et al.* 2005). A microtubule-binding Hook3 was also proposed to participate in defining the architecture and localization of the Golgi (Walenta *et al.* 2001). Another candidate was a Golgi-localized binding partner for cytoplasmic dynein, Bicaudal-D (Hoogenraad *et al.* 2001), which was proven to function mainly in a microtubule-dependent recycling pathway from the trans-Golgi network to the ER (Young *et al.* 2005). Therefore, molecules involved in the interaction between microtubules and the steady-state Golgi stacks still remain elusive. We have demonstrated that CG-NAP was dissociated from the Golgi by the on-ice treatment (Fig. 1 and 2), indicating the microtubule-dependency in its localization to the steady-state Golgi. Under this condition localization of the Golgi matrix protein GM130 was also affected but far less than that of CG-NAP (Fig. 1). This sharp sensitivity of CG-NAP may reflect its involvement in the interface between microtubules and the steady-state Golgi stacks. The interaction of CG-NAP with microtubules might be mediated by cytoplasmic dynein as is the case during transport along microtubules. However, addition of the antibody m70.1, which recognizes dynein intermediate chain and blocks dynein-mediated binding to microtubules (Young *et al.* 2000), affected the binding of CG-NAP to microtubules only slightly (our unpublished results), suggesting that intact cytoplasmic dynein is not required for this interaction. We assume that interaction of CG-NAP with microtubules at steady-state Golgi is mediated by p150^{Glued} alone or dynactin

complex, although we cannot exclude the possibility of its direct interaction with microtubules. In addition, it was reported that the Golgi is a microtubule-organizing organelle (Chabin-Brion *et al.* 2001), and we have previously shown that CG-NAP serves as microtubule nucleation sites by anchoring γ -TuRC at centrosomes (Takahashi *et al.* 2002). Therefore another possibility is that CG-NAP functions as an interface by nucleating short microtubules near the Golgi that are connected to the preexisting microtubule arrays and the Golgi stacks via some microtubule-associated proteins as was proposed for the function of GMAP-210 (Rios *et al.* 2004).

It was reported that treatment of cells at low temperature (5°C) induces PKA dissociation from the Golgi to cytosol but not from the centrosomes (Martin *et al.* 1999), which is very similar to the behavior of CG-NAP, suggesting that CG-NAP is a responsible AKAP at the Golgi. Recently, it was also reported that PKA activity plays a relevant role in the assembly and maintenance of a continuous Golgi ribbon from separated membrane stack (Bejarano *et al.* 2006). Taken together with the results of RNA interference study (Larocca *et al.* 2004), these observations suggest that CG-NAP recruited to and maintained at the Golgi is involved in the formation of Golgi ribbon as a major AKAP and/or as an interface between microtubules and the Golgi.

In summary, we have demonstrated that CG-NAP is recruited to the minus ends of microtubules by cytoplasmic dynein and localized to the steady-state Golgi apparatus in a microtubule-dependent manner, and possibly, participates in the biogenesis and maintenance of the Golgi structural integrity.

Experimental Procedures

Construction of Expression Plasmids

Mammalian expression plasmids for CG-NAP deletion mutants were constructed by inserting the corresponding cDNA fragments into pTB701-FLAG (Takahashi *et al.* 1999). cDNAs of p150^{Glued} and p50 dynamitin were cloned by PCR using HeLa Marathon-Ready cDNA library (Clontech) with appropriate primers and subcloned into pTB701-HA and pcDNA3.1 Myc-His (Invitrogen). FLAG-tagged deletion mutants were fused with mitochondrial targeting sequence, amino acid residues 16-30 of D-AKAP1 at its amino-terminus (Ma and Taylor 2002), and subcloned into pcDNA3 (Invitrogen).

Cell Culture, Transfection and Treatments

COS7, HEK293T, and HeLa cells were grown in Dulbecco's modified Eagle's medium supplemented with 10 % heat-inactivated fetal bovine serum, 50 units/ml penicillin, and 50 µg/ml streptomycin at 37 °C in a humidified 5 % CO₂ atmosphere. COS7 cells were transfected with expression plasmids by electroporation using GenePulser II (Bio-Rad), HeLa and HEK293T cells were transfected using TransIT LT-1 Transfection Reagent (Mirus).

To depolymerize microtubules cells were placed on ice for 30 minutes in the presence of 25 mM HEPES (pH7.3). To repolymerize microtubules the cells were incubated again at 37°C for appropriate time points (we referred as 'recovery' process). For acetate treatment COS7 cells were treated with Ringers acetate, pH 6.4 (80 mM NaCl, 70 mM sodium acetate, 10 mM HEPES, 10 mM glucose, 5 mM KCl, 2 mM CaCl₂, 2 mM NaPO₄, 1 mM MgCl₂) for 15 minutes in 37 °C as described previously (Vaughan *et al.* 1999). The cells were washed with PBS twice and incubate with pre-warmed medium at 37 °C for appropriate periods.

Antibodies

Polyclonal antibody to CG-NAP (αEE) was described previously (Takahashi *et al.* 1999).

Polyclonal antibodies to GRASP65 (Sutterlin *et al.* 2002) and golgin 97 (Yoshimura *et al.* 2004) were kindly provided by Dr. Vivek Malhotra (University of California San Diego) and Dr. Nobuhiro Nakamura (Kanazawa University), respectively. The following antibodies were purchased: anti- α -tubulin DM1A, rabbit anti-FLAG, mouse anti-FLAG clone M2 (Sigma); rat anti-hemagglutinin (HA) clone 3F10, mouse anti-HA clone 12CA5 (Roche Diagnostics); anti-GM 130, anti-p150^{Glued}, p50 dynamitin (BD Biosciences); mouse anti-beta actin (Abcam); mouse anti-dynein intermediate chains, rhodamine or fluorescein isothiocyanate (FITC)-conjugated secondary antibody (Chemicon International); and mouse anti-c-myc clone 9E10, horseradish peroxidase-conjugated secondary antibodies (Santa Cruz Biotechnology).

Immunofluorescence Microscopy

Cells grown on cover glasses were fixed with cold methanol at -20°C for 5 minutes. To visualize microtubule associated proteins clearly, cells were briefly extracted with 0.1% Triton X-100 for 2 minutes in a buffer consisting of 50 mM piperazine-1, 4-bis (2-ethanesulfonic acid) /KOH at pH 6.9, 5 mM MgCl₂, and 1 mM EDTA prior to fixation. Fixed cells were rehydrated with PBS, blocked with 5 % (Cardone *et al.* 2002) normal donkey serum or 5 % (w/v) BSA in Ca²⁺, Mg²⁺-free phosphate buffered saline (PBS) containing 0.1 % Triton X-100, and incubated with the relevant antibody at room temperature for 2 hours or at 4°C overnight. Then the primary antibodies were visualized by incubation with appropriate secondary antibodies conjugated with either rhodamine or FITC at room temperature for 1 hour. DNA was visualized by incubating with 4', 6-diamidino-2-phenylindole dihydrochloride (DAPI). Mitochondria were visualized using Mito Tracker Red CMXRos (Molecular probes) according to manufacture's instructions, then fixed with 4 % paraformaldehyde in 0.1 M phosphate buffer, pH 7.2. Fixed cells were permeabilized using 0.1 % Triton X-100. The fluorescence of rhodamine and FITC was

observed under a fluorescence microscope (Zeiss, Oberkochen, Germany) equipped with a CCD camera (Hamamatsu Photonics, Hamamatsu, Japan).

Immunoprecipitation and Immunoblotting

Cells were lysed in a lysis buffer consisting of 50 mM Tris-HCl at pH 7.5, 1 % Nonidet P-40, 150 mM NaCl, 1 mM EDTA, 10 µg/ml leupeptin, 1 mM PMSF and 1 mM dithiothreitol at 4 °C for 30 minutes. After centrifugation, the supernatants were incubated with appropriate antibodies at 4 °C for 2 hours. Then Protein A-Sepharose beads (GE healthcare) were added and incubated for further 30 minutes. The beads were washed with the same buffer three times, and the bound proteins were processed for immunoblotting.

Microtubule Binding Assays

Cells were lysed in a buffer consisting of 100 mM PIPES at pH 6.9, 1 mM EGTA, 1 mM MgCl₂ (PEM), and 1 % Triton X-100 at 4 °C for 30 minutes and centrifuged at 100,000 × g for 30 minutes. Microtubule binding experiments were performed according to Balczon *et al* with slight modifications. In brief, cell lysates (100 µg) were mixed with 0.5 mM GTP with or without 20 µM taxol, and then incubated for 20 minutes at 37 °C. Lysates were overlaid on a cushion of PEM buffer containing 20 % sucrose, 0.5 mM GTP with or without 10 µM taxol and followed by centrifugation at 30,000 × g for 30 minutes at 25°C. Microtubule pellets were washed, and collected with sample buffer. Bound proteins were separated by SDS-PAGE and processed for immunoblotting.

Acknowledgments

This work was supported in part by research grants from the Japan Society for the Promotion of Science, and "The 21st Century Center of Excellence" program of the Ministry of Education, Culture, Sports, Science and Technology, Japan.

References

- Allan, V. (1996) Motor proteins: a dynamic duo. *Curr.Biol.* **6**, 630-633.
- Barr, F.A. & Egerer, J. (2005) Golgi positioning: are we looking at the right MAP? *J.Cell Biol.* **168**, 993-998.
- Bejarano, E., Cabrera, M., Vega, L., Hidalgo, J., & Velasco, A. (2006) Golgi structural stability and biogenesis depend on associated PKA activity. *J.Cell Sci.* **119**, 3764-3775.
- Burkhardt, J.K. (1998) The role of microtubule-based motor proteins in maintaining the structure and function of the Golgi complex. *Biochim.Biophys.Acta* **1404**, 113-126.
- Burkhardt, J.K., Echeverri, C.J., Nilsson, T., & Vallee, R.B. (1997) Overexpression of the dynamitin (p50) subunit of the dynactin complex disrupts dynein-dependent maintenance of membrane organelle distribution. *J.Cell Biol.* **139**, 469-484.
- Cardone, L., de Cristofaro, T., Affaitati, A., Garbi, C., Ginsberg, M.D., Saviano, M., Varrone, S., Rubin, C.S., Gottesman, M.E., Avvedimento, E.V., & Feliciello, A. (2002) A-kinase anchor protein 84/121 are targeted to mitochondria and mitotic spindles by overlapping amino-terminal motifs. *J.Mol.Biol.* **320**, 663-675.
- Chabin-Brion, K., Marceiller, J., Perez, F., Settegrana, C., Drechou, A., Durand, G., & Pous, C. (2001) The Golgi complex is a microtubule-organizing organelle. *Mol.Biol.Cell* **12**, 2047-2060.
- Echeverri, C.J., Paschal, B.M., Vaughan, K.T., & Vallee, R.B. (1996) Molecular characterization of the 50-kD subunit of dynactin reveals function for the complex in chromosome alignment and spindle organization during mitosis. *J.Cell Biol.* **132**, 617-633.
- Gill, S.R., Schroer, T.A., Szilak, I., Steuer, E.R., Sheetz, M.P., & Cleveland, D.W. (1991) Dynactin, a conserved, ubiquitously expressed component of an activator of vesicle motility mediated by cytoplasmic dynein. *J.Cell Biol.* **115**, 1639-1650.
- Gillingham, A.K. & Munro, S. (2000) The PACT domain, a conserved centrosomal targeting motif in the coiled-coil proteins AKAP450 and pericentrin. *EMBO Rep.* **1**, 524-529.
- Heuser, J. (1989) Changes in lysosome shape and distribution correlated with changes in cytoplasmic pH. *J.Cell Biol.* **108**, 855-864.
- Holleran, E.A., Karki, S., & Holzbaur, E.L. (1998) The role of the dynactin complex in intracellular motility. *Int.Rev.Cytol.* **182**, 69-109.

- Holzbaur,E.L., Hammarback,J.A., Paschal,B.M., Kravit,N.G., Pfister,K.K., & Vallee,R.B. (1991) Homology of a 150K cytoplasmic dynein-associated polypeptide with the *Drosophila* gene Glued. *Nature* **351**, 579-583.
- Hoogenraad,C.C., Akhmanova,A., Howell,S.A., Dortland,B.R., De Zeeuw,C.I., Willemsen,R., Visser,P., Grosveld,F., & Galjart,N. (2001) Mammalian Golgi-associated Bicaudal-D2 functions in the dynein-dynactin pathway by interacting with these complexes. *EMBO J.* **20**, 4041-4054.
- Karcher,R.L., Deacon,S.W., & Gelfand,V.I. (2002) Motor-cargo interactions: the key to transport specificity. *Trends Cell Biol.* **12**, 21-27.
- Karki,S. & Holzbaur,E.L. (1999) Cytoplasmic dynein and dynactin in cell division and intracellular transport. *Curr.Opin.Cell Biol.* **11**, 45-53.
- Keryer,G., Di Fiore,B., Celati,C., Lehtreck,K.F., Mogensen,M., Delougee,A., Lavia,P., Bornens,M., & Tassin,A.M. (2003) Part of Ran is associated with AKAP450 at the centrosome: involvement in microtubule-organizing activity. *Mol.Biol.Cell* **14**, 4260-4271.
- King,S.M. (2000) The dynein microtubule motor. *Biochim.Biophys.Acta* **1496**, 60-75.
- Larocca,M.C., Shanks,R.A., Tian,L., Nelson,D.L., Stewart,D.M., & Goldenring,J.R. (2004) AKAP350 interaction with cdc42 interacting protein 4 at the Golgi apparatus. *Mol.Biol.Cell* **15**, 2771-2781.
- Ma,Y. & Taylor,S. (2002) A 15-residue bifunctional element in D-AKAP1 is required for both endoplasmic reticulum and mitochondrial targeting. *J.Biol.Chem.* **277**, 27328-27336.
- Martin,M.E., Hidalgo,J., Vega,F.M., & Velasco,A. (1999) Trimeric G proteins modulate the dynamic interaction of PKAII with the Golgi complex. *J.Cell Sci.* **112 (Pt 22)**, 3869-3878.
- Nishimura,T., Takahashi,M., Kim,H.S., Mukai,H., & Ono,Y. (2005) Centrosome-targeting region of CG-NAP causes centrosome amplification by recruiting cyclin E-cdk2 complex. *Genes Cells* **10**, 75-86.
- Parton,R.G., Dotti,C.G., Bacallao,R., Kurtz,I., Simons,K., & Prydz,K. (1991) pH-induced microtubule-dependent redistribution of late endosomes in neuronal and epithelial cells. *J.Cell Biol.* **113**, 261-274.
- Rios,R.M. & Bornens,M. (2003) The Golgi apparatus at the cell centre. *Curr.Opin.Cell Biol.* **15**, 60-66.
- Rios,R.M., Sanchis,A., Tassin,A.M., Fedriani,C., & Bornens,M. (2004) GMAP-210 recruits gamma-tubulin complexes to cis-Golgi membranes and is required for Golgi ribbon formation.

Cell **118**, 323-335.

Schmidt,P.H., Dransfield,D.T., Claudio,J.O., Hawley,R.G., Trotter,K.W., Milgram,S.L., & Goldenring,J.R. (1999) AKAP350, a multiply spliced protein kinase A-anchoring protein associated with centrosomes. *J.Biol.Chem.* **274**, 3055-3066.

Schroer,T.A. & Sheetz,M.P. (1991) Two activators of microtubule-based vesicle transport. *J.Cell Biol.* **115**, 1309-1318.

Sillibourne,J.E., Milne,D.M., Takahashi,M., Ono,Y., & Meek,D.W. (2002) Centrosomal anchoring of the protein kinase CK1delta mediated by attachment to the large, coiled-coil scaffolding protein CG-NAP/AKAP450. *J.Mol.Biol.* **322**, 785-797.

Sutterlin,C., Hsu,P., Mallabiabarrena,A., & Malhotra,V. (2002) Fragmentation and dispersal of the pericentriolar Golgi complex is required for entry into mitosis in mammalian cells. *Cell* **109**, 359-369.

Takahashi,M., Shibata,H., Shimakawa,M., Miyamoto,M., Mukai,H., & Ono,Y. (1999) Characterization of a novel giant scaffolding protein, CG-NAP, that anchors multiple signaling enzymes to centrosome and the golgi apparatus. *J.Biol.Chem.* **274**, 17267-17274.

Takahashi,M., Yamagiwa,A., Nishimura,T., Mukai,H., & Ono,Y. (2002) Centrosomal proteins CG-NAP and kendrin provide microtubule nucleation sites by anchoring gamma-tubulin ring complex. *Mol.Biol.Cell* **13**, 3235-3245.

Tynan,S.H., Purohit,A., Doxsey,S.J., & Vallee,R.B. (2000) Light intermediate chain 1 defines a functional subfraction of cytoplasmic dynein which binds to pericentrin. *J.Biol.Chem.* **275**, 32763-32768.

Vaughan,K.T., Tynan,S.H., Faulkner,N.E., Echeverri,C.J., & Vallee,R.B. (1999) Colocalization of cytoplasmic dynein with dynactin and CLIP-170 at microtubule distal ends. *J.Cell Sci.* **112** (Pt 10), 1437-1447.

Vaughan,P.S., Miura,P., Henderson,M., Byrne,B., & Vaughan,K.T. (2002) A role for regulated binding of p150(Glued) to microtubule plus ends in organelle transport. *J.Cell Biol.* **158**, 305-319.

Walenta,J.H., Didier,A.J., Liu,X., & Kramer,H. (2001) The Golgi-associated hook3 protein is a member of a novel family of microtubule-binding proteins. *J.Cell Biol.* **152**, 923-934.

Waterman-Storer,C.M., Karki,S., & Holzbaur,E.L. (1995) The p150Glued component of the dynactin complex binds to both microtubules and the actin-related protein centractin (Arp-1). *Proc.Natl.Acad.Sci.U.S.A* **92**, 1634-1638.

Witczak,O., Skalhegg,B.S., Keryer,G., Bornens,M., Tasken,K., Jahnsen,T., & Orstavik,S. (1999) Cloning and characterization of a cDNA encoding an A-kinase anchoring protein located in the centrosome, AKAP450. *EMBO J.* **18**, 1858-1868.

Yoshimura,S., Yamamoto,A., Misumi,Y., Sohda,M., Barr,F.A., Fujii,G., Shakoori,A., Ohno,H., Mihara,K., & Nakamura,N. (2004) Dynamics of Golgi matrix proteins after the blockage of ER to Golgi transport. *J.Biochem.(Tokyo)* **135**, 201-216.

Young,A., Dictenberg,J.B., Purohit,A., Tuft,R., & Doxsey,S.J. (2000) Cytoplasmic dynein-mediated assembly of pericentrin and gamma tubulin onto centrosomes. *Mol.Biol.Cell* **11**, 2047-2056.

Young,J., Stauber,T., del Nery,E., Vernos,I., Pepperkok,R., & Nilsson,T. (2005) Regulation of microtubule-dependent recycling at the trans-Golgi network by Rab6A and Rab6A'. *Mol.Biol.Cell* **16**, 162-177.

Legends to Figures

Figure 1 CG-NAP localizes to the Golgi apparatus in a microtubule- dependent manner.

(A) HeLa cells were fixed with methanol and stained with anti-CG-NAP and anti- α -tubulin antibodies. (a, b) Control cells, (c, d) cells placed on ice for 30 minutes, and (e, f) cells after 20 minutes recovery from the on ice treatment. (g, h) In control or on-ice treated cells, the Golgi apparatus was visualized with anti-GM130 antibody. Bars, 20 μ m. (B) Cells were placed on ice for 30 minutes in the presence of taxol (+Tx) (i, j), or cells were recovered for 20 minutes from the on-ice treatment in the presence of nocodazole (+Nz) (k, l). Bar, 20 μ m.

Figure 2 CG-NAP associates with microtubules.

(A) Subcellular localization of CG-NAP during recovery from the on-ice treatment. At indicated time points during recovery from the on-ice treatment cells were extracted with 0.1% Triton X-100 prior to fixation with methanol, and then triple stained with anti-CG-NAP, anti- α -tubulin antibodies and DAPI. Merged images were indicated by green (α -tubulin), red (CG-NAP) and blue (DAPI). Bar, 10 μ m. (B) HeLa cell lysates were mixed with GTP and taxol and incubated at 37°C for 20 minutes. Polymerized microtubules were precipitated by centrifugation, and proteins in the microtubule pellet (MT ppt), unbound supernatants (MT sup) and 10 % of used lysates (input) were separated by SDS-PAGE followed by immunoblot with antibodies against CG-NAP, GMAP210, p150^{Glued}, α -tubulin and β -actin. β -actin was used as a negative control. (C) Schematic representation of CG-NAP and its deletion mutants used in this work. Positions of the deletion mutants are shown with amino acid residues on the left sides. (D) Lysates of the COS7 cell expressing FLAG-tagged deletion mutants were incubated at 37°C as described in (B), with (+) or without (-) 20 μ M taxol. Microtubule-bound (ppt) or unbound (sup) fractions were probed for the presence of deletions with anti-FLAG antibody (upper panel). The presence of

α -tubulin and β -actin was also monitored (lower panel).

Figure 3 CG-NAP colocalizes with dynein-dynactin subunits during recovery from the on-ice treatment.

COS7 cells at 4 minutes after recovery from the on-ice treatment were extracted with Triton X-100 prior to fixation with methanol, followed by immunostaining with anti-CG-NAP in combination with anti- α -tubulin, anti-dynamitin, anti-DIC, or anti-p150^{Glued} antibodies respectively. Bar, 20 μ m.

Figure 4 CG-NAP colocalizes with dynein-dynactin subunits during recovery from acetate treatment.

(A) Control COS7 cells, (B) cells treated with acetate solution for 15 minutes, and (C) cells at 4 minutes or (D) at 30 minutes after removing acetate were briefly extracted with Triton X-100 and fixed with methanol. The cells were immunostained with antibodies against CG-NAP and α -tubulin or dynamitin, or GM130. Nuclei were visualized with DAPI. Bars, 10 μ m.

Figure 5 CG-NAP associates with dynactin subunit p150^{Glued}.

(A) Association of endogenous CG-NAP with p150^{Glued}. HeLa cell lysates (input) were immunoprecipitated with anti-CG-NAP antibody (CG-NAP IP) or control antibody (control IP), followed by immunoblotting with anti-p150^{Glued} or anti-CG-NAP antibody. (B) Association of recombinant CG-NAP with p150^{Glued}. COS7 cells lysates (input) expressing FLAG-CG-NAP and HA-p150^{Glued} were immunoprecipitated with anti-FLAG antibody (FLAG IP) or control antibody (control IP), followed by immunoblotting with anti-HA or anti-FLAG antibody. (C) Association of deletion mutants of CG-NAP with p150^{Glued}. FLAG-tagged deletion mutants were cotransfected with HA-tagged p150^{Glued} into COS7 cells,

and then lysates (input) were immunoprecipitated with anti-FLAG (FLAG IP, left panels), anti-HA (HA IP, right panels) or control antibodies (ctr IP), followed by immunoblotting with anti-HA or anti-FLAG antibodies. PVDF filter in the left panel was probed with anti-HA and then reprobed with anti-FLAG without stripping the anti-HA antibody. Asterisk indicates HA-p150^{Glued} probed with anti-HA antibody. Arrow on the right panel indicates non-specific band detected by anti-FLAG antibody.

Figure 6 CG-NAP₁₂₂₉₋₂₄₄₄ interacts with functional cytoplasmic dynein complex.

(A) Subcellular localization of CG-NAP deletion mutants. FLAG-tagged mutants were expressed in COS7 cells for 16 hours, and then the cells were fixed with methanol and immunostained with anti-FLAG antibody. Bar, 10μm. (B) Effect of expression of Mt-tagged deletion mutants on the mitochondrial distribution (see Experimental Procedures). Mt-tagged deletions of CG-NAP were expressed in COS7 cells. Subcellular localization of the deletions and mitochondria were visualized by anti-FLAG antibody (left panels) and Mitotracker (right panels), respectively. Bar, 10μm. (C) Association of CG-NAP₁₂₂₉₋₂₄₄₄ with microtubules. COS7 cell lysates expressing FLAG-tagged deletion mutants were incubated at 37°C as described in Fig. 2D. Microtubule-bound (ppt) or unbound (sup) fractions were probed for the presence of deletions and microtubules with anti-FLAG antibody (upper panel) and α-tubulin antibody (lower panel), respectively. (D) Association of CG-NAP₁₂₂₉₋₂₄₄₄ with p150^{Glued}. FLAG-tagged deletion mutants were cotransfected with HA-tagged p150^{Glued} into COS7 cells, and then lysates (input) were immunoprecipitated with anti-FLAG (FLAG IP) or control antibodies (ctr IP), followed by immunoblotting with anti-HA or anti-FLAG antibodies.

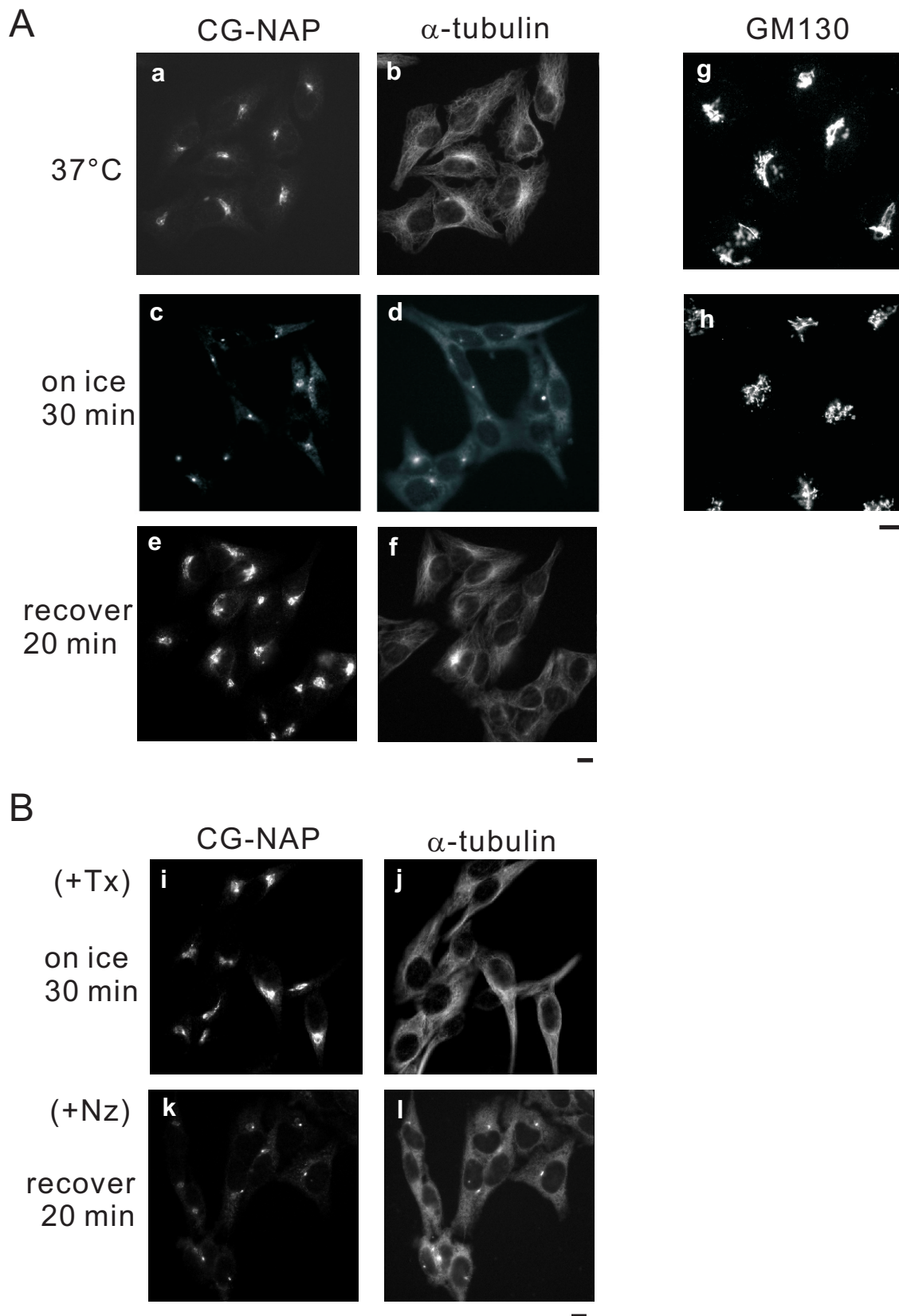
Figure 7 Overexpression of CG-NAP₁₂₂₉₋₂₄₄₄ causes fragmentation of the Golgi apparatus similar to that of dynamitin.

(A) Effect of overexpression of FLAG-tagged CG-NAP₁₂₂₉₋₂₄₄₄ on the Golgi structure.

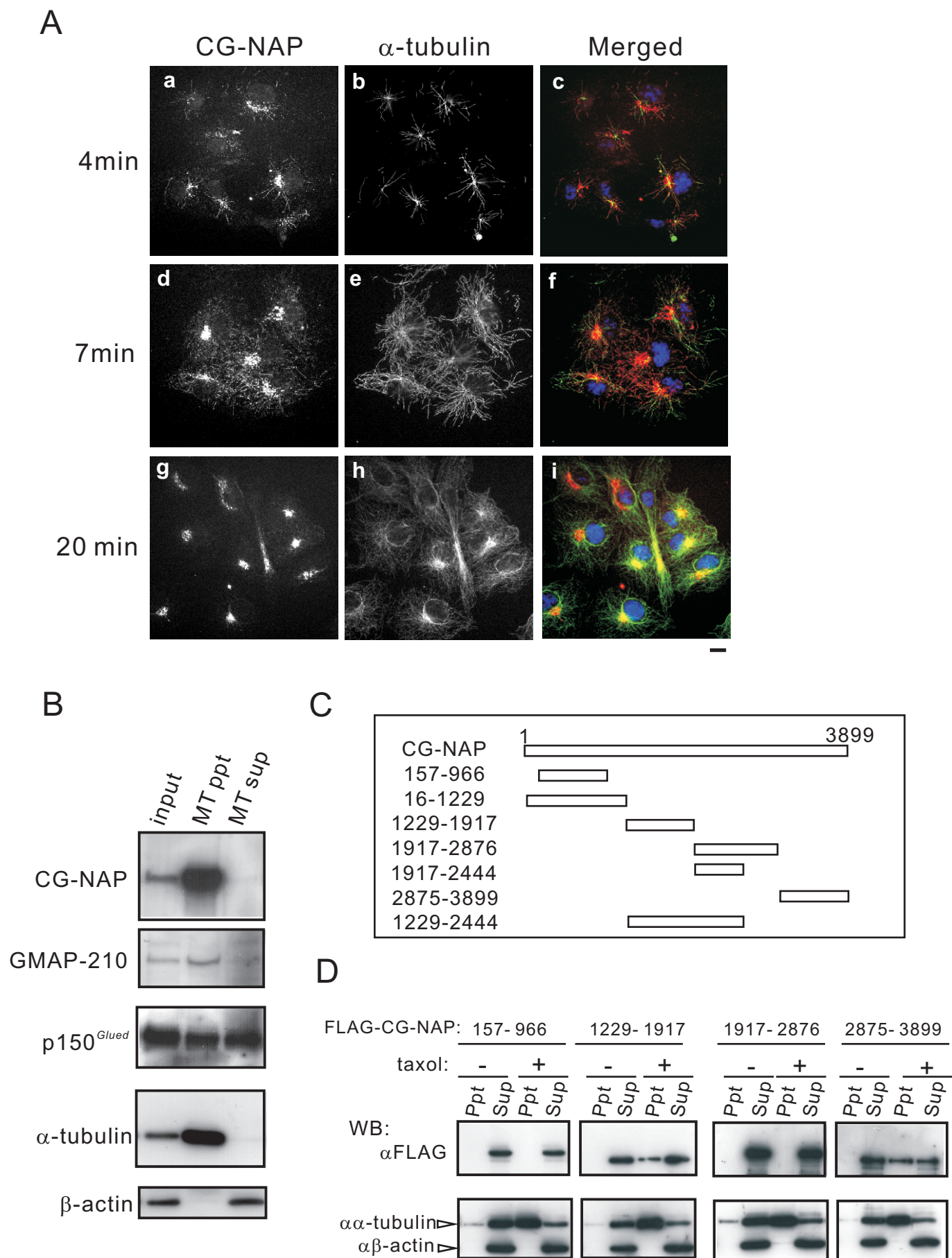
FLAG-CG-NAP₁₂₂₉₋₂₄₄₄ was overexpressed in COS7 cells for 36 hours, and double stained with anti-FLAG and anti-GM130 or anti-golgin 97 and anti-GM130 antibodies. Expressing cells are indicated with white arrows. Merged images were shown with GM130 in green, golgin 97 in red and nuclei in blue. The inset shows expanded image of scattered Golgi elements marked by white box. Bars, 10 μ m. (B) Effect of overexpression of myc-tagged

dynamitin (dynamitin-myc) on the Golgi structure. Dynamitin-myc was overexpressed in COS7 cells, and double stained with anti-myc and anti-GRASP 65 or anti-golgin 97 and anti-GM130 antibodies. Bars, 10 μ m. (C) Effect of overexpression of FLAG-tagged

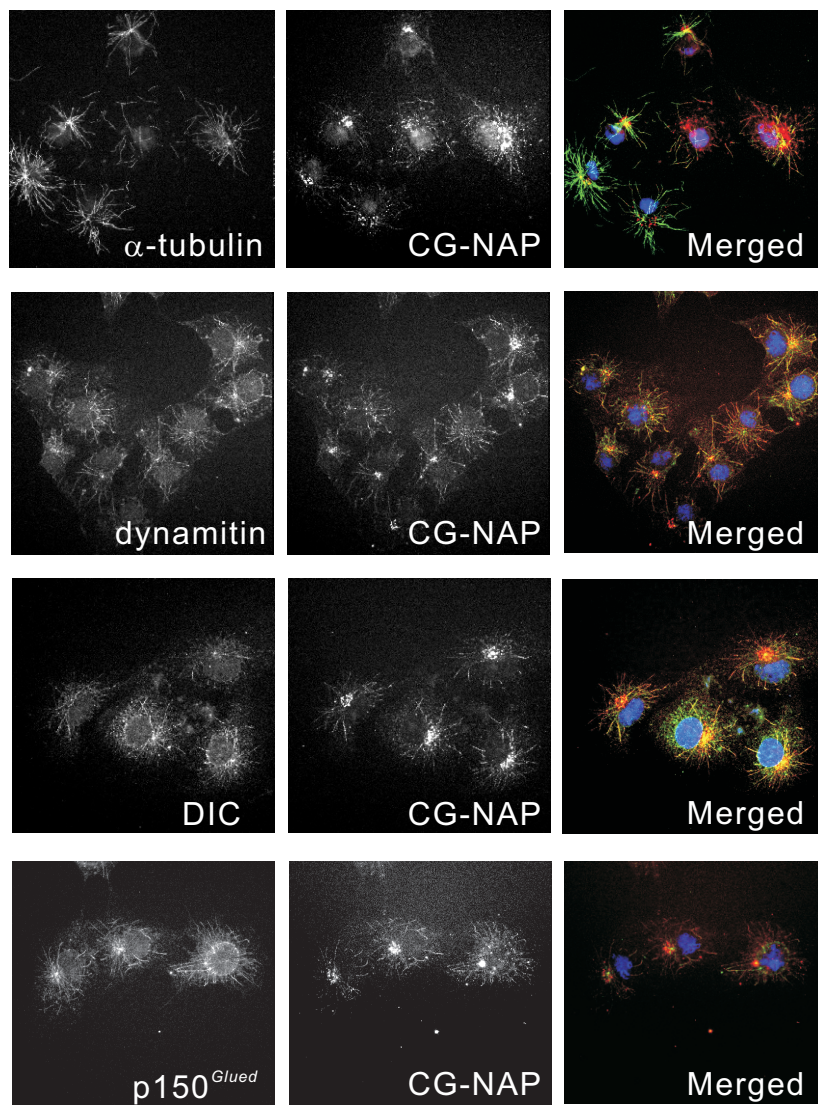
CG-NAP₁₂₂₉₋₂₄₄₄ (upper panel) or dynamitin-myc (lower panel) on microtubule-associated p150^{Glued}. FLAG-CG-NAP₁₂₂₉₋₂₄₄₄ or dynamitin-myc was overexpressed in COS7 cells for 36 hours, and double stained with anti-golgin 97 and anti-p150^{Glued} antibodies. White arrows indicate the cells expressing FLAG-CG-NAP₁₂₂₉₋₂₄₄₄ or dynamitin-myc. The right panels show the expanded image of the area marked by white box. Bars, 10 μ m.



Kim, *et al.* Figure 1.

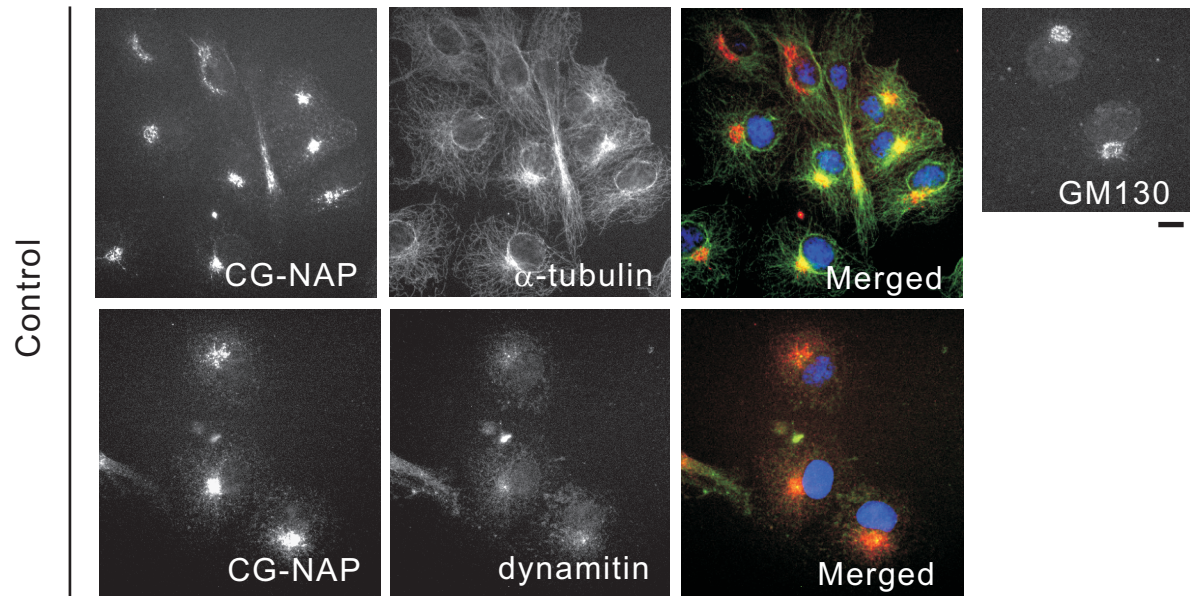


Kim, *et al.* Figure 2.

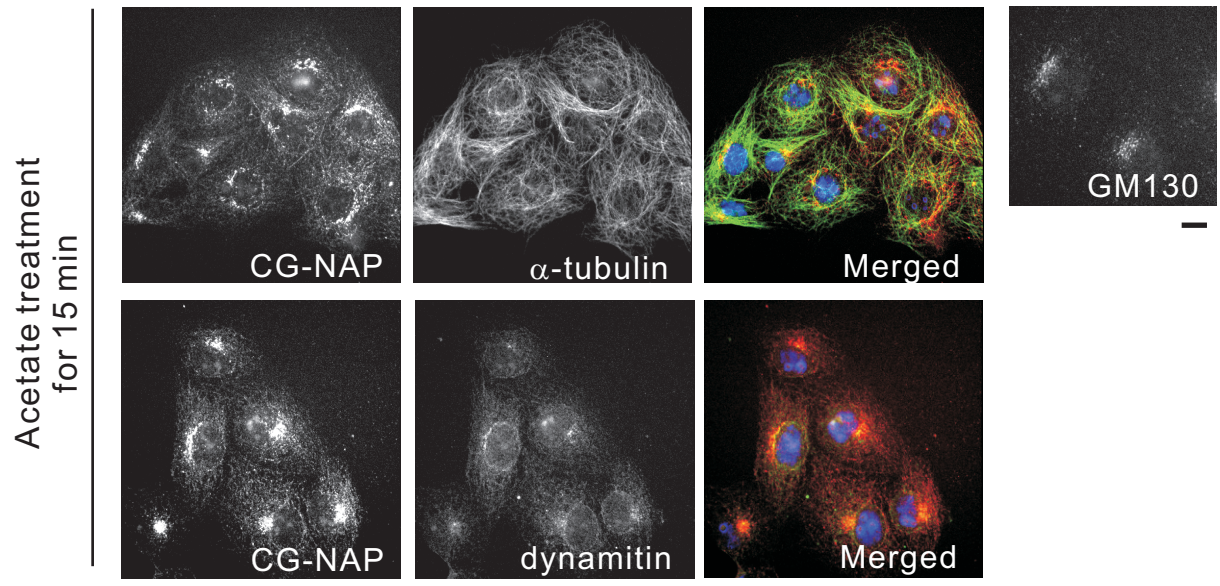


Kim, *et al.* Figure 3.

A

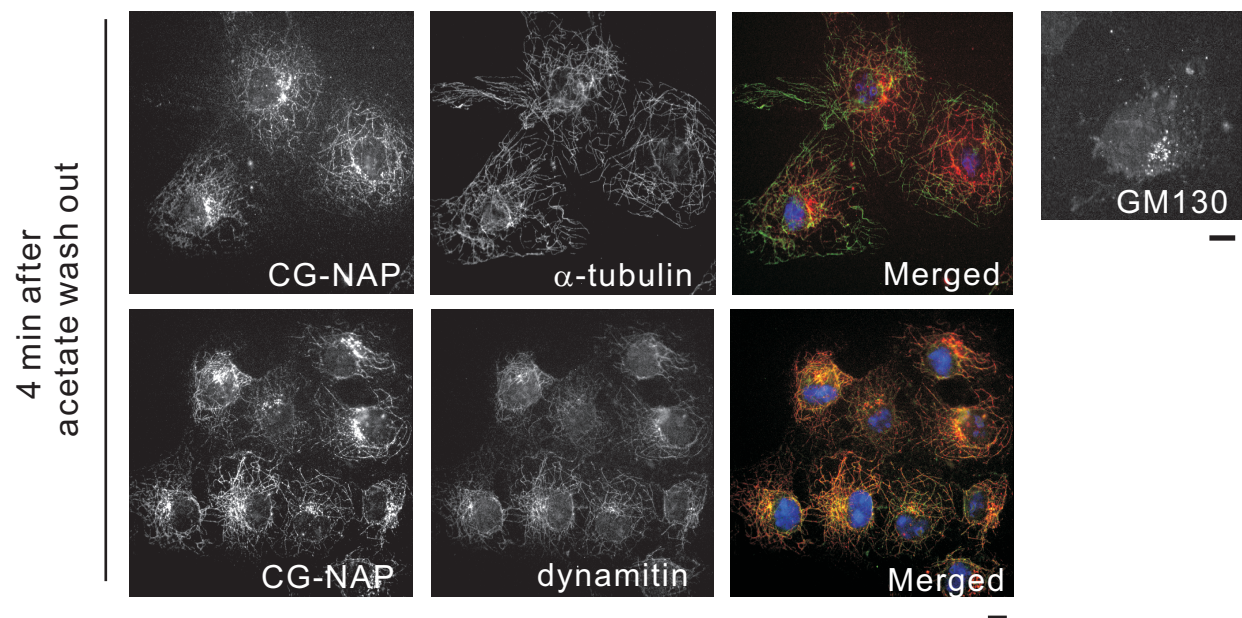


B

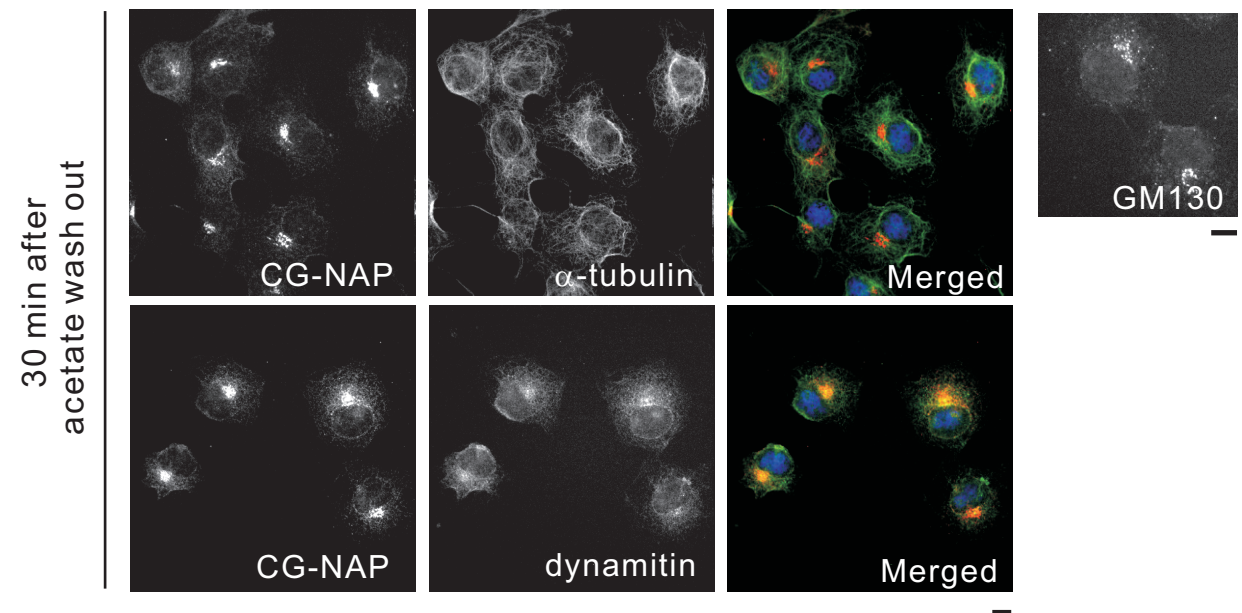


Kim, *et al.* Figure 4.

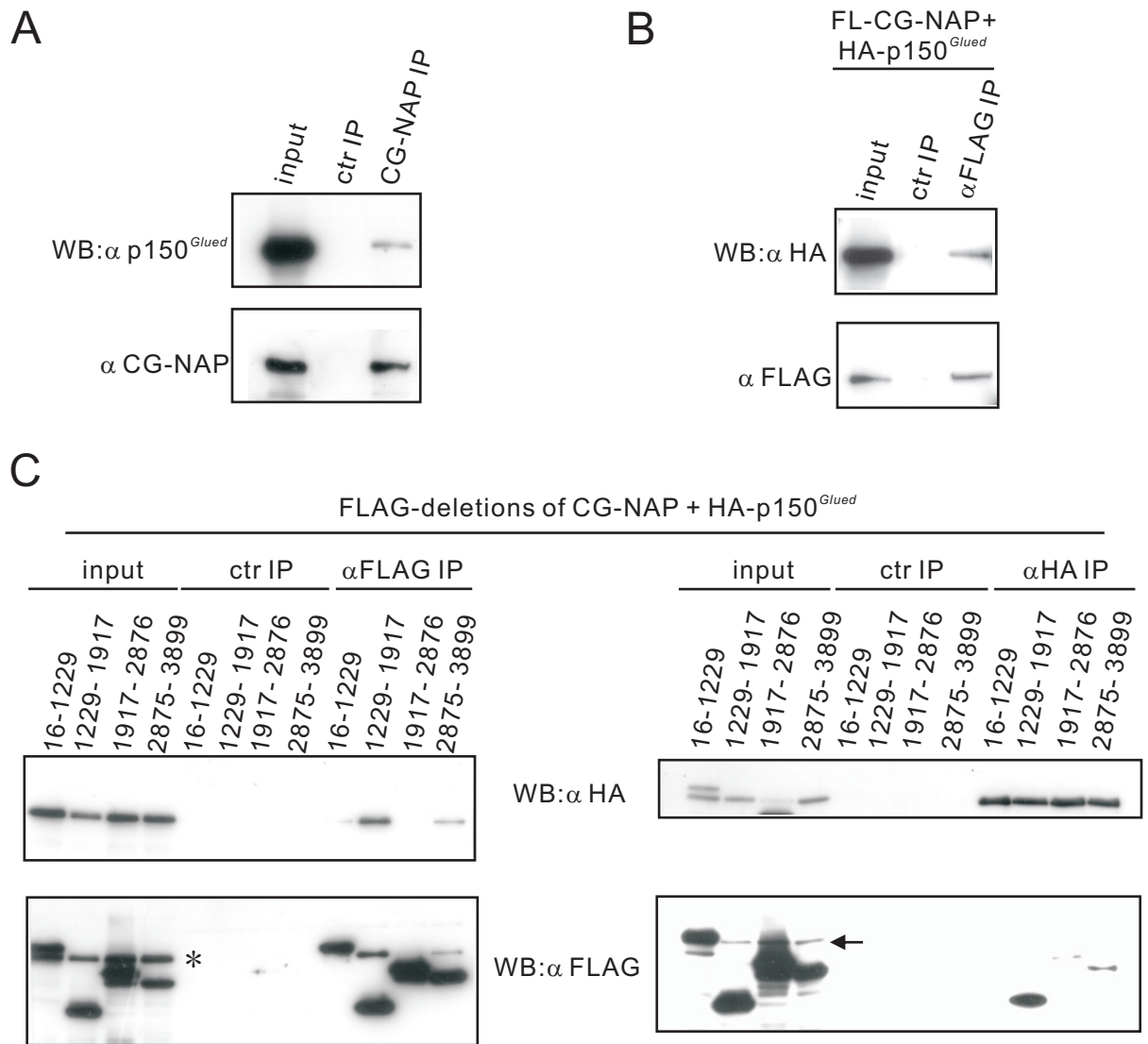
C



D



Kim, *et al.* Figure 4., continued

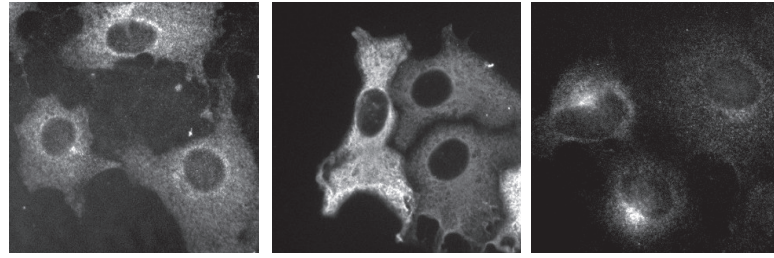


Kim, *et al.* Figure 5.

A

FLAG-CG-NAP: 1229-1917 1917-2444 1229-2444

α FLAG

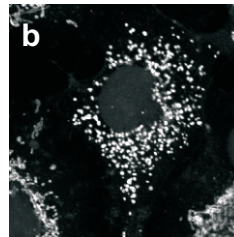
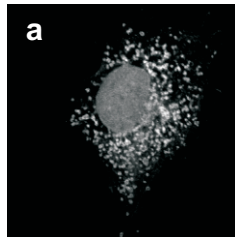


B

EGFP

Mito Tracker

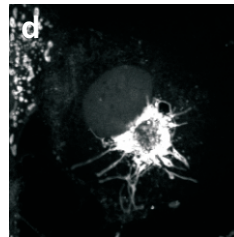
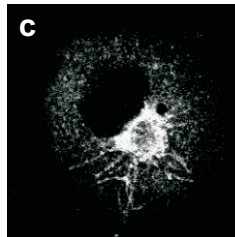
Mt-EGFP



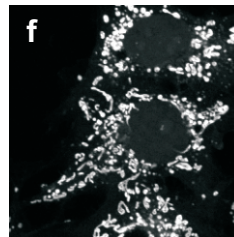
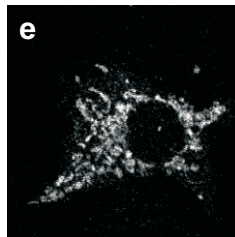
α FLAG

Mito Tracker

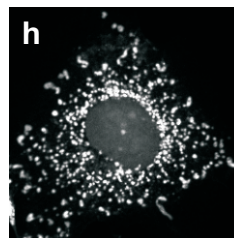
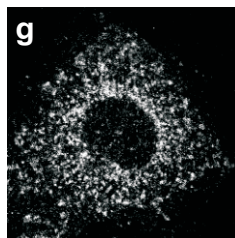
Mt-FLAG-CG-NAP:
1229-2444



1229-1917



1917-2444

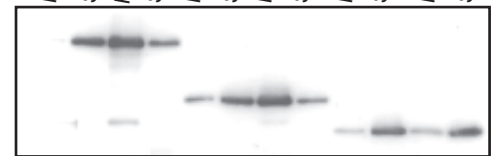


C

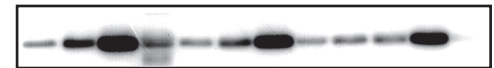
FLAG-CG-NAP: 1229-2444 1229-1917 1917-2444

taxol: - + - + - +
Ppt Sup Ppt Sup Ppt Sup Ppt Sup Ppt Sup Ppt Sup

WB: α FLAG

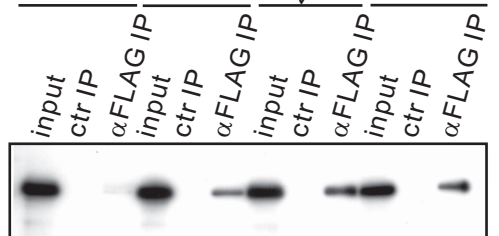


WB: α α -tubulin



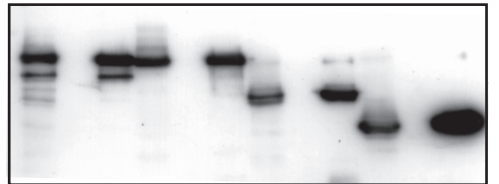
D

16-1229 1229-2444 2875-3899 1229-1917



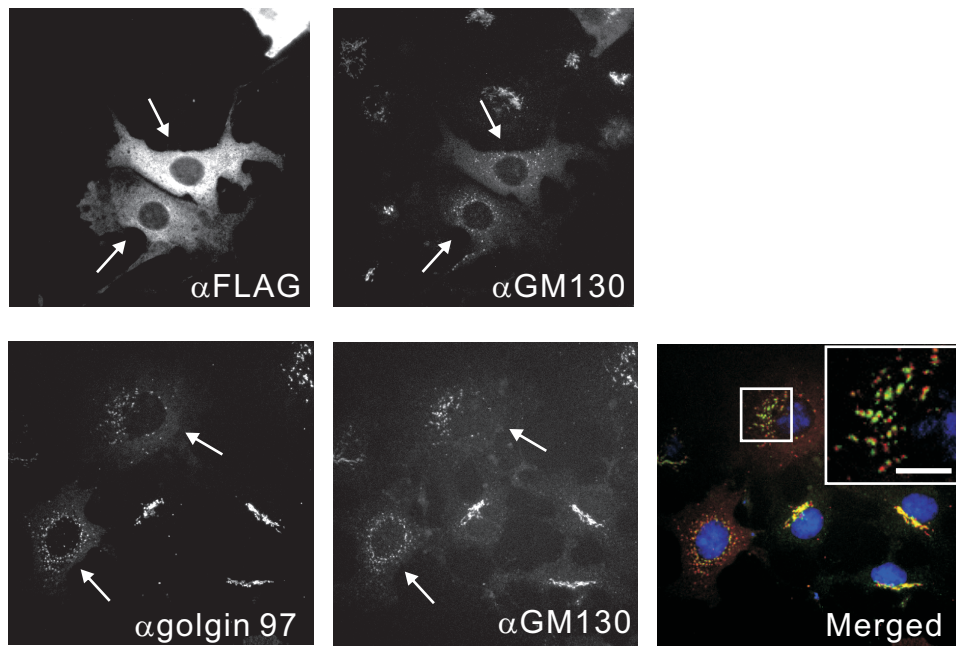
WB: α HA

WB: α FLAG

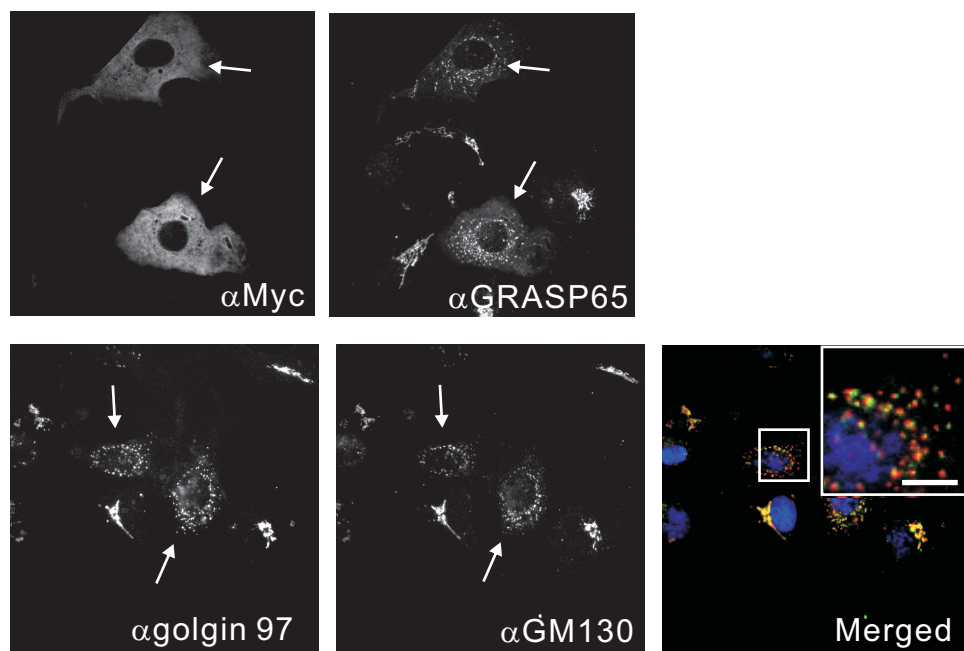


Kim, *et al.* Figure 6.

A FLAG-CG-NAP₁₂₂₉₋₂₄₄₄ expression



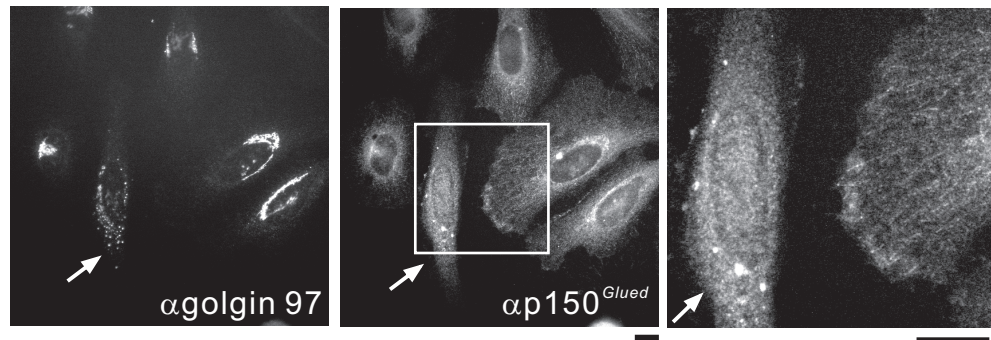
B Dynamitin-Myc expression



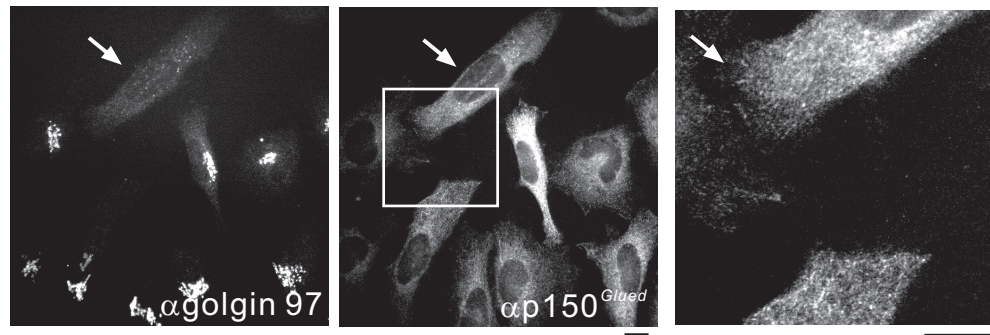
Kim, *et al.* Figure 7.

C

FLAG-CG-NAP₁₂₂₉₋₂₄₄₄ expression



Dynamitin-Myc expression



Kim, *et al.* Figure 7., continued